Geological Society, London, Special Publications

Ultrasonic wave velocities as a diagnostic tool for the quality assessment of marble

T. Weiss, P. N. J. Rasolofosaon and S. Siegesmund

Geological Society, London, Special Publications 2002, v.205; p149-164.
doi: 10.1144/GSL.SP.2002.205.01.12

Notes

Ultrasonic wave velocities as a diagnostic tool for the quality assessment of marble

T. WEISS[1], P. N. J. RASOLOFOSAON[2] & S. SIEGESMUND[1]

[1] *Geowissenschaftliches Zentrum der Georg-August-Universität Göttingen, Goldschmidtstrasse 3, D-37077 Göttingen, Germany (e-mail: tweiss@gwdg.de)*

[2] *Institut Français du Petrole, Geophysics Department, Rock Physics Laboratory, 1 et 4 avenue de Bois Preau, 92852 Rueil Malmaison Cedex, France*

Abstract: Marbles are frequently used as building stones even if they mostly show a limited durability. Thus, different marbles with different fabric types and states of preservation have been investigated in order to constrain the interaction between fabric, state of deterioration and ultrasonic wave velocities. Experimental data reveal that the state of preservation of a marble is clearly documented by ultrasonic wave velocities of compressional waves. For a maximum porosity of up to 1% velocities determined on dry samples range from about 1 km s^{-1} to over 6 km s^{-1}. Anisotropy of ultrasonic wave velocities is a common feature of marbles due to a lattice preferred orientation of the anisotropic rock-forming minerals calcite and dolomite. Pre-existing and thermally induced microcracks tend to increase this anisotropy. For Lasa marble, this increase can be explained by a coincidence of intrinsic anisotropy and the effect of pre-existing and thermally induced microcracks. For many marbles, velocities are reduced to at about 1 km s^{-1} as a consequence of thermal degradation due to only one heating cycle up to 100°C. Model calculations reveal that the velocity reduction is caused by cracks with an extremely small aspect ratio of about 0.005 or even less. The porosity associated with this very early stage of deterioration will not be increased significantly and thus, thermal degradation cannot be determined by other petrophysical measurements.

Sculptures and monuments made of marble are often subjected to strong degradation within a limited time span. The final stage of this weathering is frequently characterized by a granular disintegration of the marble, i.e. the cohesion between the grains is completely lost (Fig. 1). In the initial stage of weathering, thermally induced microcracks are thought to play an important role in degradation (Widhalm *et al.* 1996; Siegesmund *et al.* 2000). They are caused or enhanced by the strong directional dependence of the thermal dilatation coefficient α of calcite (Fig. 2). When the thermal stresses exceed the threshold of cohesion between adjacent grains microcracks are formed (e.g. Tschegg *et al.* 1999; Weiss *et al.* 2002).

To avoid the complete loss of some culturally and historically important buildings or monuments and the tremendous costs of conservation or replacement of degraded marbles, more elaborate methods to detect structural disintegration are required. For many years ultrasonic measurements have been used as a non-destructive tool for the quality assessment of marble and other building stones (Duerrast *et al.* 1999; Snethlage *et al.* 1999). The basic assumption is that a decrease in the velocity of compressional waves (Vp) is correlated with a certain stage of deterioration of a marble. A classification of the state of deterioration of Carrara marble and an empirically derived correlation function between Vp and porosity, presented by Köhler (1991), is shown in Table 1.

In order to understand the relationship between ultrasonic wave velocities, porosity and type of pore fluid in the present investigation the interaction between the microfabric and the ultrasonic wave velocities is re-evaluated using the Lasa marble as a particular example. A comprehensive compilation of the behaviour of different commercially used marble types is used to describe differences in the ultrasonic wave velocity diagnostics as a consequence of varying microfabric types and different degrees of weathering. Furthermore, selected marbles are thermally altered to constrain magnitude and directional dependence of thermal degradation. In our investigations we focus on compressional wave velocities since they are widely used for both on-site inspections and laboratory studies.

From: SIEGESMUND, S., WEISS, T. & VOLLBRECHT, A. 2002. *Natural Stone, Weathering Phenomena, Conservation Strategies and Case Studies*. Geological Society, London, Special Publications, **205**, 149–164.
0305-8719/02/$15.00

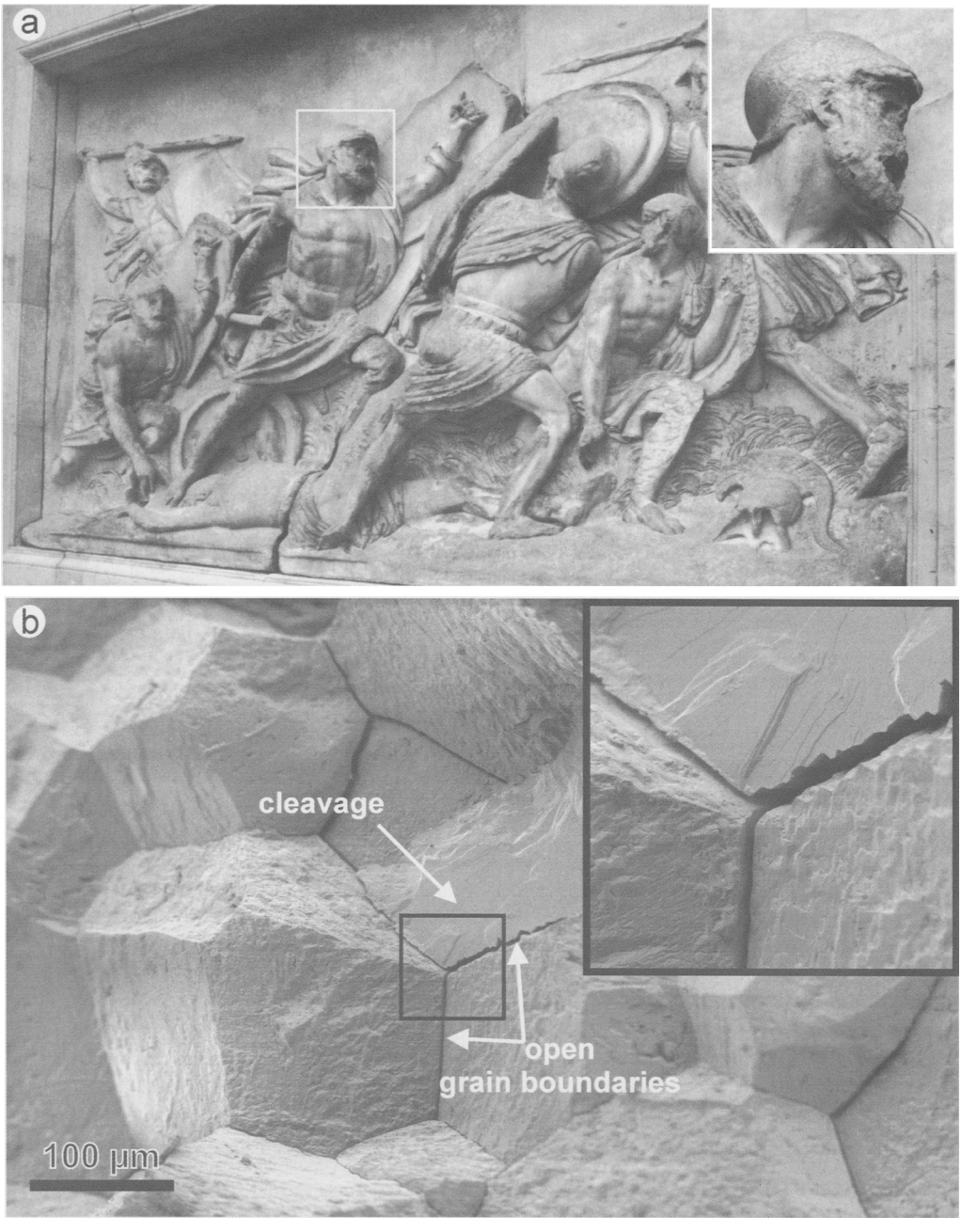

Fig. 1. Degradation of marble. (**a**) A relief from the Siegestor in Munich (Germany) showing granular disintegration; (**b**) SEM images of a fracture plane in Carrara marble showing decohesion along the grain boundaries and fractures along cleavage planes.

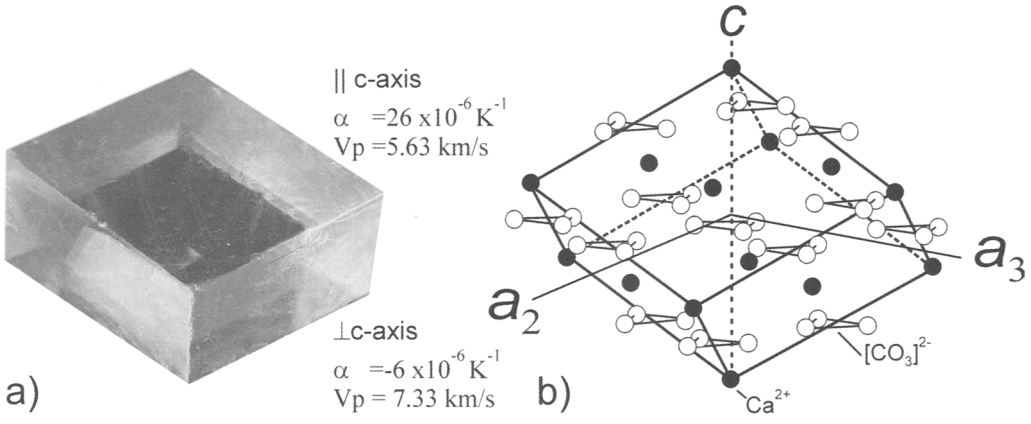

Fig. 2. Single crystal properties of calcite. (**a**) Calcite cleavage rhombohedron with the coefficients of thermal expansion (after Kleber 1959) and ultrasonic wave velocities (Dandekar 1968) parallel and perpendicular to the crystallographic c-axis; (**b**) calcite structure with respect to the calcite crystallography (c-axis and a-axes).

Table 1. *State of deterioration of Carrara marble based on ultrasonic velocity measurements (after Köhler 1991)*

Damage class	*Vp* (km s^{-1})	Condition
0	> 5.0	fresh
I	3.0–5.0	increasingly porous
II	2.0–3.0	granular disintegration
III	1.5–2.0	fragile
IV	< 1.5	crumbling rock

Fundamentals

Anisotropy of elastic properties

A more or less pronounced directional dependence of almost all petrophysical properties is observed for natural building stones (Siegesmund 1996). Thus, anisotropy is rather the rule than an exception and must be taken into account for all natural building stones. In particular marbles may show a pronounced anisotropy, even if their composition is relatively simple. It is caused by the strong single crystal anisotropy of calcite (Fig. 2) and/or dolomite, the main rock-forming minerals in marble, in combination with their lattice preferred orientation (here referred to as texture) and volume content. The intrinsic properties can be overprinted by extrinsic factors like pre-existing microcracks and porosity caused or enhanced by weathering.

The elastic wave propagation is different in porous and non-porous media (e.g. Bourbié *et al.* 1987). At first glance, marbles can be treated as non-porous materials since their initial porosity is mostly very small (Ruedrich *et al.* 2001). The interaction of anisotropic crystals leads to a more or less anisotropic behaviour of the bulk rock depending on the texture. With a given single crystal anisotropy, the bulk rock anisotropy may vary accordingly from almost random, for a rock with a weak texture, to strongly anisotropic, for a rock with a pronounced texture. When extrinsic parameters (e.g. pores, microcracks) are present, in particular ultrasonic wave velocity propagation is affected (Christensen 1965). The velocities of ultrasonic wave velocities (*Vp*) are mostly lowered, even if this phenomenon depends on the type of pore fluid (see discussion below).

Relationship between porosity and Vp

Even if the initial porosity of a marble is mostly very small, pre-existing microcracks have an important effect on physical properties (Weiss *et al.* 2001). They result from a complex geological history and may show a uniform distribution or a directional dependence. During weathering, the porosity increases and the resulting material has clearly to be treated as porous. This new porosity can be uniformly distributed or directionally dependent.

There are different theoretical approaches describing the elastic behaviour of cracked or porous materials. The main methods for computing the elastic properties of a heterogeneous material, i.e. a material containing minerals, cracks and different pore fluids, can be classified into the following overall categories.

The first category of methods ignores the geometry of the pore space. Associated methods just average some simple physical parameters like travel-time (Wyllie *et al.* 1956, 1958), stiffness (Voigt 1928) and compliance (Reuss 1929), even if there exist more sophisticated ones (Hashin-Strikman bounds; Hashin 1981). These methods either are applicable to restricted types of rocks (e.g. sedimentary rocks with average to large primary porosity) or give only rough estimates of the overall elastic parameters, especially when the rock exhibits compliant features (cracks, microfractures, etc.) and when its constituents have contrasted stiffnesses (e.g. mineral grains and saturating fluids).

Another category assumes specific geometries for the pores (spherical, ellipsoidal, disc-shaped etc.). One of the most commonly used and accepted method in this group is that of O'Connell & Budiansky (1974). The method, a self-consistent method, is predictive and determines the effect of each heterogeneity (pores, cracks, grains etc.) taking into account the presence of the surrounding heterogeneities and their interactions.

There also exist methods to quantify the effect (magnitude and directional dependence) of extrinsic parameters on ultrasonic wave propagation. Here we use the method proposed by Arts *et al.* (1996) and applied to natural rocks by Rasolofosaon *et al.* (2000). The method considers the elastic properties of the rock sample under various confining pressure conditions. With increasing confining pressure microcracks are closed. The difference between the elastic compliances of the rock under high and ambient pressure leads to a quantitative microcrack characterization, using mathematical derivation based on strict mechanical principles (Rasolofosaon *et al.* 2000). The same procedure can be used to determine the difference in compliance between a water-saturated and a dry sample or to quantify the effect of thermally induced microcracks. The inversion process provides the additional compliance, more precisely the normalized compliance, due to the presence of the cracks and its directional dependence. The normalized compliance is the ratio (in per cent) between the compliance of the cracks and the compliance of the rock matrix. Note that the compliance of the cracks is proportional to the crack density (number of cracks per unit length) multiplied by the compliance of a single crack. As a consequence, from a mechanical point of view, a few very compliant cracks and many weakly compliant cracks would have the same effect with this approach.

Experimental methods

Fabric-induced anisotropy

In order to understand a rock's behaviour it is essential to gather as much information as possible on the rock's structure, since there is a complex interaction between the rock fabric and petrophysical properties as compiled by Siegesmund (1996). Thus, qualitative and quantitative description of critical fabric parameters is indispensable. A qualitative fabric description is obtained by transmitted light microscopy using standard thin sections. Quantified fabric data are determined by digital image analysis giving information on grain size, grain size distributions, grain shape and shape preferred orientations. The amount of pre-existing microcracks is obtained by the measurement of microcracks using a universal stage. Since special emphasis is placed on the directional dependence of ultrasonic wave velocities, all investigations are carried out on at least three mutually perpendicular directions or sections. All data are related to an orthogonal reference system (x, y, z), defined with respect to macroscopic and microscopic features like lineation and foliation. In this coordinate frame, the xy-plane is the plane parallel to a foliation, the x-direction is the direction of the lineation. When no macroscopic fabric elements were found an arbitrary reference system is defined.

Determination of ultrasonic wave velocities

For the ultrasonic measurements spherical rock samples with a diameter of 50 mm and an accuracy of 0.02 mm have been prepared. Spherical samples allow the determination of an arbitrary anisotropy pattern. This becomes important when the symmetry of the anisotropy pattern is not associated with the reference coordinate system, i.e. when the maximum or minimum velocity does not coincide with the x-, y- or z-direction determined macroscopically.

Transient times of ultrasonic pulses (piezoceramic transducers, resonant frequency 0.5 MHz) were measured in 90 directions using the pulse transmission technique at ambient conditions

(Birch 1960). With a given diameter, the velocities of compressional waves (Vp) can be calculated. The measurements were performed at dry (Vp_{dry}) and completely water-saturated (Vp_{sat}) samples to simulate different sample conditions. Furthermore, specimens were heated up to 100°C to force thermal degradation after the samples had been measured at water-saturated and dry sample conditions. The heating was performed at a rate of about 1°C min^{-1} to ensure continuous thermal equilibration of the samples and comparability with other thermal degradation measurements (e.g. Zeisig *et al.* 2002).

At low confining pressures, velocities are the result of an intrinsic and extrinsic part. With increasing confining pressure, microcracks are closed and their reducing effect on the ultrasonic wave velocities vanishes. Thus, Vp measurements in the present study have also been performed under hydrostatic pressure. For these measurements, (i) spheres (50 mm diameter) and (ii) cylindrical samples (length and diameter 30 mm) have been used. Cylindrical samples give more accurate data on absolute velocity values, since the coupling of the transducers on the specimen surface is less problematic than on spherical samples. All specimens were orientated according to the x-, y- and z-direction of the structural reference frame. The porosity of the marbles was determined by buoyancy weighting of the spheres used for the ultrasonic measurements.

Results

Origin and microfabric of the marbles investigated

Marbles from different localities in Italy (Carrara and Lasa) and Poland (Kauffung, Prieborn, Grosskunzendorf) have been used for the investigations. Their fabric properties are shown in detail in Weiss *et al.* (1999; except Lasa marble) and are summarized in Table 2. Some of the specimens are directly from the quarry (fresh samples), while the weathered ones were previously used on buildings and had been replaced on-site. The different marbles cover a broad range of textures, microfabrics and weathering states (Weiss *et al.* 1999). All of the marbles, with the exception of the Kauffung marble, are more or less pure calcitic marbles. The Kauffung marble has dolomitic veins predominantly parallel to the macroscopically visible metamorphic foliation (Weiss *et al.* 1999). Some of the marbles show an equilibrated microstructure with straight grain boundaries (microstructural Type I). Others show serrated grain boundaries (Type II), or a bimodal grain size distribution with small recrystallized and large relict grains with irregular grain boundaries (Type III), or a microstructure with evidence for grain boundary migration (Type IV). Of course, the classification into four fabric types requires some simplification of the naturally very heterogeneous rock fabric. Thus, the prevailing presence of one of the above-mentioned fabric characteristics does not necessarily exclude the others.

Intrinsic versus extrinsic anisotropy

The Lasa marble may be used as a case study for the variations of ultrasonic velocities at different sample conditions in dependence on the rock fabric. The sample is directly from the quarry and, thus, comprises characteristics gathered from its geological and processing (quarrying) history. It exhibits a serrate microfabric (Type II, Fig. 3a–c) and a weak texture with c-axis (006) maximum of about 1.8 mrd and a-axis [110] maximum of 1.3 mrd (Fig. 3d,e) (mrd = multiples of random distribution). The c-axes show a slight girdle tendency (Fig. 3d).

The Vp_{min} at water-saturated condition parallels the maximum of the c-axis concentration and the Vp_{max} the maximum of the a-axis concentration, respectively (Fig. 4a). The velocities cover a range between 6.3 and 6.65 km s^{-1}. Evidently, orthogonal measurements along the x-, y- and z-direction would not monitor the total anisotropy in this case, since the Lasa marble shows a Vp_{max} and Vp_{min} at oblique angles in between the x-, y-, and z-direction.

The velocity pattern determined on the dry specimen is quite similar (Fig. 4b). However, the velocities are significantly reduced, possibly due to the presence of pre-existing microcracks. By comparing measurements at water-saturated and dry sample conditions it is evident that pre-existing cracks also show a correlation with the texture. The maximum difference between Vp_{sat} and Vp_{dry} (1.8 km s^{-1}) is found parallel to the z-direction, the minimum (1.25 km s^{-1}) at an intermediate angle between the x- and y-direction (Fig. 4c). An increase in the directional dependence of Vp due to microcracks is observed, since intrinsic Vp_{min} and the maximum velocity reduction due to cracks coincide. Vp_{sat} covers the range between 6.3 and 6.65 km s^{-1} while Vp_{dry} is in the range between 4.5 and 5.4 km s^{-1}. The calculation of the normalized compliance is based on the data determined on the water-saturated and dry

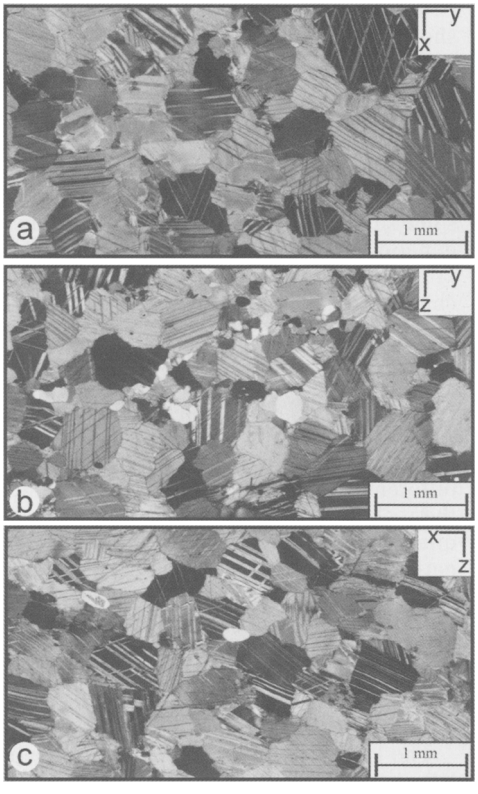

Fig. 3. Microfabric of the Lasa marble. (**a–c**) Microstructure (crossed polarizers); (**d**) c-axis (006) and (**e**) a-axis [110] pole figures (isolines in multiples of random distribution, mrd). The texture was measured by means of neutron diffraction. The reference coordinate system is indicated in c-axis pole figure; the maximum is indicated by a filled circle.

sample. It is a characteristic for pre-existing cracks, and the maximum value parallel to the z-direction (109%) is approximately twice as large as the corresponding minimum (Fig. 4c).

This effect can be understood when the microfabric is taken into account. The general shape preferred orientation of the calcite grains is weak (Fig. 5a, b). However, in the xz-section a weak shape anisotropy is observed (Fig. 5c). Grain boundaries show a preferred orientation parallel or slightly oblique to the foliation. Two sets of open microcracks, associated to e-twins (Fig. 5d) and cleavage planes (Fig. 5e), are observed for the Lasa marble. Both exhibit a maximum parallel to the z-direction, while the cleavage planes show a second maximum parallel to the x-direction (Fig. 5e). Thus, the coincidence of the aforementioned fabric properties may lead to the larger velocity difference between the water-saturated and dry sample condition parallel to the z-direction (see Fig. 4c).

Thermally-induced microcracks

After the measurement of the specimens under water-saturated and dry sample conditions, the samples were thermally treated by heating up to 100°C. All marbles except the Kauffung marble exhibit a pronounced velocity decrease of about 1 km s^{-1} as a consequence of thermal treatment (Table 2). Again the Lasa marble is used as a particular example. The directional dependence of newly generated cracks as a consequence of thermal treatment for this marble can be visualized when the pole figures for the dry and the thermally cracked sample condition are compared. Notice that the pole figures in Figures 4b and 6a represent the same measurement, while the pole figures in Figure 6b and e

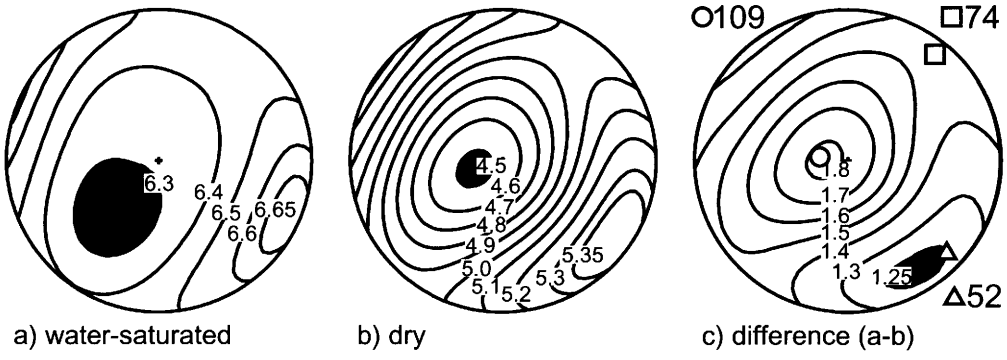

Fig. 4. Ultrasonic wave velocities in Lasa marble before thermal alteration: (**a**) at water-saturated conditions; (**b**) at dry sample conditions; and (**c**) their difference pole figure. Normalized compliances are given as a maximum (circle), intermediate (square) and minimum (triangle) value and their positions are indicated in the difference pole figure. The velocity minimum is filled in black.

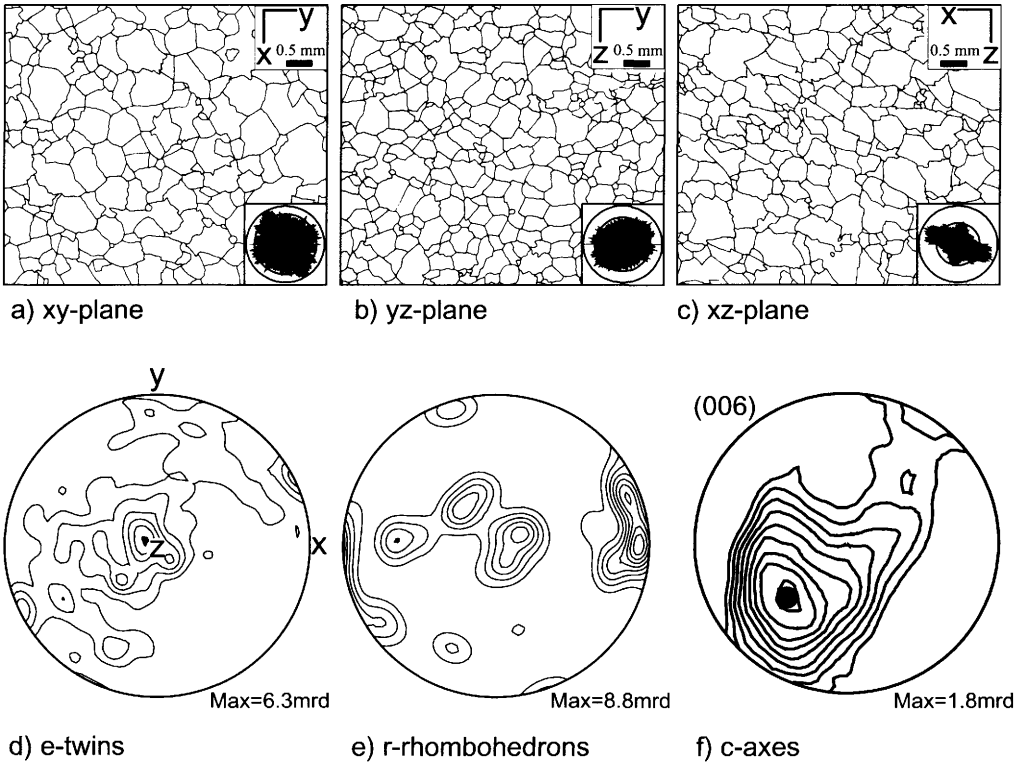

Fig. 5. Quantified fabric of Lasa marble. (**a–c**) Digitized images of the grain boundaries and their orientation (as rose diagrams) in respect to the reference coordinate system; (**d**) orientation diagram of open e-twins and (**e**) cleavage planes determined with a standard universal stage (the maximum is given in multiples of random distribution, contour interval is 1 mrd); (**f**) c-axis (006) texture, measured by neutron diffraction (contour interval is 0.1 mrd).

Table 2. *Summarized fabric properties and ultrasonic wave velocities of the investigated marbles*

Marble type	Sample condition	Approx. grain size (μm)	Micro-structure	Comp.	Φ (%)	Vp_{dry}			Vp_{sat}			Vp_{tcr}		
						Vp_{max} (km s^{-1})	Vp_{min} (km s^{-1})	A (%)	Vp_{max} (km s^{-1})	Vp_{min} (km s^{-1})	A (%)	Vp_{max} (km s^{-1})	Vp_{min} (km s^{-1})	A (%)
Lasa I	fresh	400	I/II	cc	0.43	5.10	4.42	13.30	6.48	6.19	4.46	–	–	–
Lasa II (LA)	fresh	400	II	cc	0.37	5.39	4.48	16.94	6.67	6.29	5.57	4.25	3.45	18.82
Lasa III	fresh	400	II	cc	0.38	5.39	4.61	14.62	6.50	6.09	6.35	4.60	3.64	20.87
Carrara I	fresh	95	III	cc	0.20	6.42	6.16	4.13	6.76	6.62	2.12	5.56	5.32	4.32
Carrara II (CA)	fresh	130	III	cc	0.14	6.53	6.41	6.26	6.83	6.61	3.26	5.48	5.08	7.30
Carrara III	fresh	150	I	cc	0.44	3.45	2.67	22.50	6.14	5.94	3.46	–	–	–
Carrara IV	weathered	140	I	cc	0.94	1.54	1.43	7.39	5.55	5.35	3.53	–	–	
Prieborn	weathered	150	I	cc	0.77	3.03	2.11	30.12	5.65	5.31	6.11	–	–	–
Kauffung I (KA)	fresh	80	III	cc/do	0.23	6.58	5.43	17.78	7.17	6.31	12.04	6.56	5.44	17.07
Kauffung II	weathered	80	III	cc/do	0.32	6.34	5.04	20.44	6.97	6.19	11.22	–	–	–
Kauffung III	weathered	80	III	cc/do	0.26	6.97	5.99	14.11	6.95	6.08	12.57	–	–	–
Kauffung IV	weathered	80	III	cc/do	0.27	6.72	5.84	13.05	7.00	6.19	12.57	–	–	–
Grosskunzendorf I (GK)	fresh	1500	IV	cc	0.31	5.05	4.37	13.59	6.83	6.48	5.18	4.20	3.64	13.33
Grosskunzendorf II	weathered	1500	IV	cc	0.46	4.59	3.63	20.81	6.42	6.10	5.09	–	–	–

Abbreviations: comp., composition; Φ, porosity; Vp_{dry}, Vp at dry sample conditions; Vp_{sat}, Vp at water-saturated sample conditions; Vp_{tcr}, Vp at thermally cracked sample conditions; A, anisotropy calculated as $A = ((Vp_{max} - Vp_{min})/Vp_{max}) \times 100$

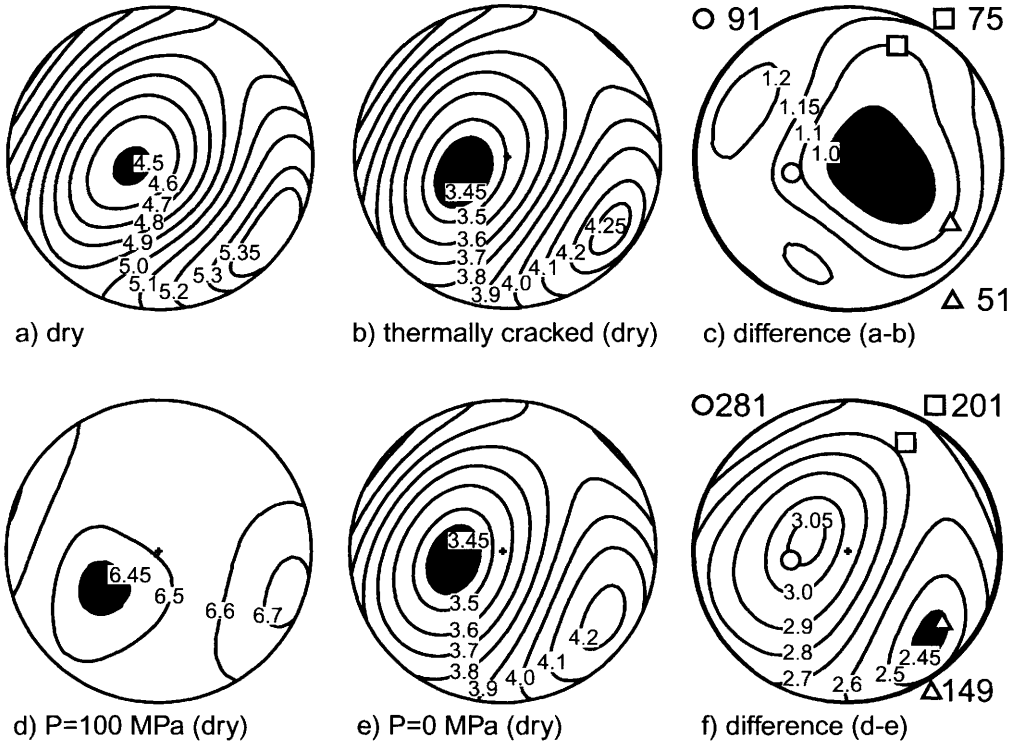

Fig. 6. Ultrasonic wave velocity measurements after thermal alteration: (**a**) at dry sample condition, (**b**) at dry but thermally cracked condition and (**c**) their difference pole figure. Measurements of the thermally altered sample; (**d**) at a confining pressure of 100 MPa, (**e**) at 0 MPa and (**f**) their difference pole figure. Velocity isolines are given in kilometres per second, the reference coordinates are the same as in Figure 3d.

are retrieved from a different experimental setup. A tremendous velocity reduction of about 1 km s^{-1} is observed after only one heating cycle up to 100°C (Fig. 6b,c). The associated difference pole figure exhibits a weak anisotropy which may explain a deviation in the pole figure pattern (compare Figs 4c and 6c). This observation indicates that the velocity reduction due to thermally induced cracks is generally more uniform. A more uniform distribution of thermally induced microcracks may be expected when grain boundary cracking is the predominant crack mechanism since the shape preferred orientation is very weak for this marble. Intergranular (grain boundary) cracking is the probable crack mechanism at these low temperatures (Fredrich & Wong 1986; Weiss *et al.* 2002). However, the directions of maximum, intermediate and minimum normalized compliance for the thermally cracked specimen still coincide with the directions of the pre-existing cracks (compare Figs 4c and 6c). Note that, after one heating cycle, the additional compliance due to thermally induced microcracks (here 91%) is in the same range as that of the pre-existing cracks. Thus, thermal degradation must be very efficient in reducing ultrasonic wave velocities.

Pressure dependence of Vp

The pressure-dependent measurements of the Lasa marble were performed on the thermally treated sample. At a confining pressure of 100 MPa (Fig. 6d) the pole figure is quite similar to the pole figure at water-saturated condition. This indicates that most of the crack porosity caused by pre-existing cracks is accessible and is stiffened by the presence of water. Thus, even the small porosity of 0.37% of the Lasa marble may be interconnected porosity. The corresponding pole figure at 0 MPa pressure (Fig. 6e) shows a good coincidence with the dry measurement shown in Figure 6b even if different

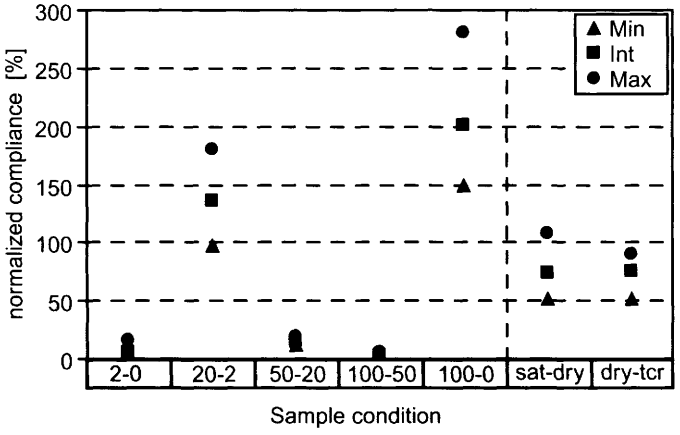

Fig. 7. Normalized compliance of the Lasa marble at different sample conditions (as indicated). The normalized compliances were calculated for incremental pressure intervals between 2 MPa and 0 MPa (2-0), 20 MPa and 2 MPa (20-2), 50 MPa and 20 MPa (50-20), 100 MPa and 50 MPa (100-50). The total value for the normalized compliance was determined from the measurement at 100 MPa and 0 MPa (100-0). Corresponding values for the difference between the water-saturated and dry sample conditions (sat-dry) and for the dry and dry but thermally cracked (dry-tcr) sample conditions are given additionally.

experimental setups were used. This may be taken as an indication that the velocity measurements using different experimental setups really give comparable data. The effect of both types of microcracks, pre-existing and thermally induced ones, can be derived from Figure 6f. The *Vp*-reduction is in the range from 2.45 to 3.05 km s^{-1} and the symmetry of the difference pole figure equals that observed in Figure 4c.

At a pressure of 100 MPa, all cracks are closed and the corresponding pole figure is characteristic for the intrinsic material properties of the Lasa marble. This is documented by the observation that the largest increase in *Vp* (i.e. a large value for the normalized compliance) is observed already at 20 MPa while it is significantly lower at the other incremental pressures (i.e. 50 MPa minus 20 MPa and 100 MPa minus 50 MPa). This means that even at a relatively small pressure of 20 MPa most of the cracks are already closed. Depending on the type of the porosity (i.e. flat cracks or round pores), a complete closure of microcracks may be reached at significantly higher confining pressures. The normalized compliance at 20 MPa is not entirely equivalent to the total amount of normalized compliance observed for the pressure difference between 100 MPa and 0 MPa (Fig. 7). Thus, an interaction of all microcracks and a reinforced effect of cracks on ultrasonic wave velocities must be expected.

A pressure-dependent increase of velocities is a general property of many marbles. Four principal types describing the interdependence between pore space and intrinsic anisotropy are shown in Figure 8. The velocities were determined on cylindrical samples cut along the x-, y- and z-direction of the structural reference frame. A strong and weak pressure-dependent increase in *Vp* can be observed for intrinsically isotropic (Fig. 8a, b) and anisotropic (Fig. 8c, d) marbles, respectively. Even marbles directly from the quarry in one region, as for example Carrara, can exhibit completely different properties (see Fig. 8a, b) as a consequence of their different fabrics (Barsotelli *et al.* 1998; Leiss & Weiss 2000). Changes in the composition (i.e. certain dolomite contents) are clearly monitored by higher ultrasonic wave velocities (Fig. 8c, d). All specimens with cracks show a strong increase of *Vp* within the first 100 MPa. Basically all calcitic marbles investigated exhibit an average velocity of about 6.7 km s^{-1} at a pressure of 200 MPa, regardless how small their Vp_{dry} may be.

Maximum velocity of water-saturated samples

The compilation of the behaviour of all marbles shown in Table 2 gives important information on the response of different marbles to water saturation. The maximum velocity of water-saturated samples (Vp_{sat}) tends to decrease with a decreasing velocity at dry (Vp_{dry}) sample conditions (Fig. 9a). The linear trend was

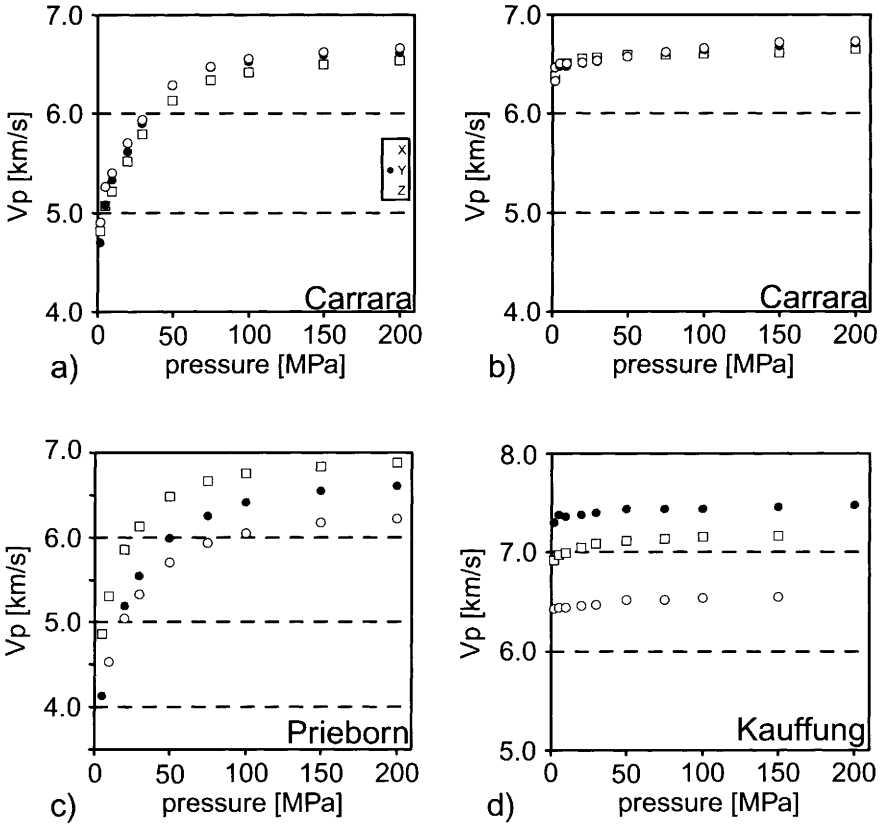

Fig. 8. Relationship between intrinsic and extrinsic anisotropy of different marbles. Relatively isotropic marbles with (**a**) a high and (**b**) a low amount of pre-existing microcracks. Anisotropic marbles with (**c**) a high and (**d**) a low amount of pre-existing microcracks. While marbles with pre-existing microcracks (a, c) show a distinct increase in *Vp* with increasing pressure, the *Vp* increase is very weak for non-cracked marbles (b, d). Note that for the first case the velocity increase with pressure vanishes at about 100 MPa indicating that most of the cracks are closed at this pressure interval. The dolomitic composition of the Kauffung marble (d) is clearly visible in higher velocities compared to the other calcite marbles.

calculated for all Vp_{max} and Vp_{min} and varies only slightly (see Fig. 9a). Some specific examples may be used to illustrate this effect. Example A (a strongly weathered Carrara marble with a porosity of 0.97%), shows a weak anisotropy (A) at both water-saturated and dry sample conditions (Fig. 9b); Vp_{dry} varies from 1.43 to 1.54 km s^{-1} (A = 7.1%) and Vp_{sat} from 5.35 to 5.55 km s^{-1} (A = 3.6%). In contrast, example B (a Prieborn marble with a porosity of 0.77%) shows a higher variation in velocities at dry sample conditions than at water-saturated sample conditions: Vp_{dry} varies from 2.11 to 3.03 km s^{-1} (A = 30.12%) and Vp_{sat} from 5.31 to 5.65 km s^{-1} (A = 6.11%). Both specimens show a similar microstructure with straight grain boundaries (polygonal fabric; Weiss *et al.* 1999) but remarkable differences in the behaviour of ultrasonic wave velocities.

All individual velocity directions, determined on one sample, follow the trend which was calculated for all marbles. This effect is also evident for example C (the fresh Lasa marble with a porosity of 0.37%), even if the velocities at dry sample conditions are significantly higher compared to example B. Most of the marbles rapidly leave the curve characterizing the coincidence of Vp_{sat} and Vp_{dry}. An exceptional example for a marble with a very small initial porosity and a very small degree of degradation is shown with example D. This specimen, a marble from Kauffung in Poland with a porosity of 0.23%, shows a coincidence of Vp_{dry} and Vp_{sat}. The anisotropy of Vp varies according to

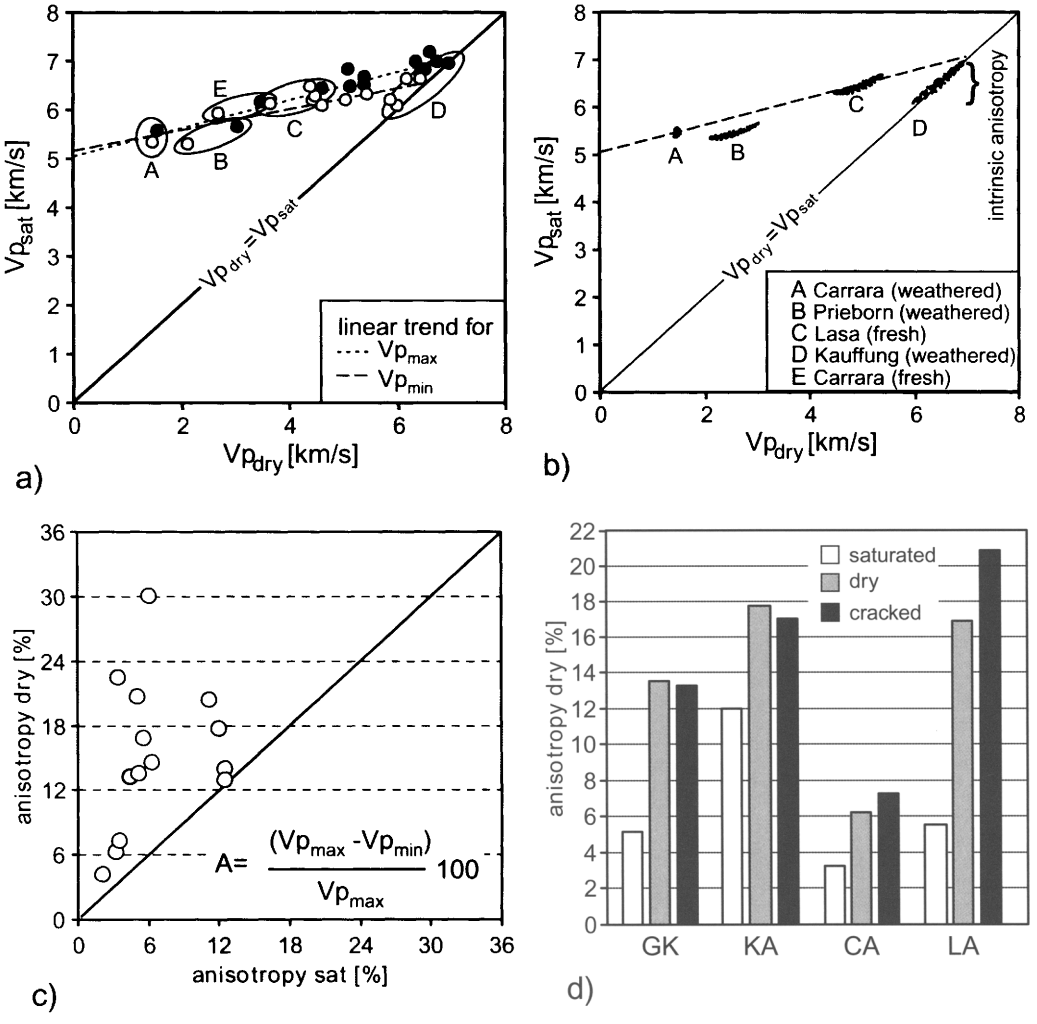

Fig. 9. Ultrasonic wave velocities in marbles. (**a**) Velocities at water-saturated sample conditions (Vp_{sat}) as a function of velocities at dry sample conditions (Vp_{dry}). Different specific examples (A–E, see (b) for description) described in the text are outlined. A linear trend has been calculated for all maximum (black circles) and minimum (white circles) Vp. (**b**) For selected examples all Vp data determined on spherical samples are shown for all measured directions. (**c**) Anisotropy (A) of the samples as a function of water-saturation. (**d**) Change in anisotropy due to thermal cracking (for abbreviations see Table 2).

the strong texture of this marble from 12.04% at water-saturated to 17.78% at dry sample conditions and only a small deviation from the curve ($Vp_{sat} = Vp_{dry}$) is observed (Weiss *et al.* 2001). Due to the strong anisotropy of this marble, a pronounced directional dependence of thermal dilatation has to be expected. Another marble with extraordinary properties is shown by example E. This Carrara marble is fresh from the quarry and has a porosity of 0.44%. However, Vp_{dry} is already very low covering the range between 2.67 and 3.45 km s^{-1} even if Vp_{sat} is relatively high (5.94 to 6.14 km s^{-1}). The anisotropy of this marble is relatively low at water-saturated sample conditions (3.46%) and very large at dry sample conditions (22.5%). Moreover, Ruedrich *et al.* (2001) have shown that this marble has, compared to other Carrara marbles, a higher propensity for thermal degradation.

Anisotropies in dry marbles may vary from 4% to 30% (Fig. 9c). When the marbles are

water-saturated, they cover a significantly smaller range between 3% and 12%. A thermal degradation may reinforce or reduce the anisotropy in marble leading to a higher (CA and LA) or lower (GK and KA) anisotropy of thermally cracked specimens calculated as percentages, respectively (Fig. 9d). However, these values have to be handled with care. A velocity difference of 1 km s^{-1} in a marble with Vp_{max} = 7.0 km s^{-1} and Vp_{min} = 6 km s^{-1} gives an anisotropy of A = 14.29% while the same velocity difference in a marble with Vp_{max} = 3.0 km s^{-1} and Vp_{min} = 2 km s^{-1} gives an anisotropy of A = 33.33%. If it is assumed that a homogeneously degraded marble shows an overall velocity reduction of 1 km s^{-1} at all sample directions its final anisotropy crucially depends on the initial (intrinsic) anisotropy. The final anisotropy may be larger even if there is a uniform degradation.

Model calculations

In order to find constraints for the magnitude and shape of the pore space in marble we modelled the velocity reduction as a function of crack geometry using the well known theoretical prediction of O'Connell & Budiansky (1974). The basic principle is that a given porosity is formed by certain types of ellipsoidal cracks. The crack geometry is only defined by the aspect ratio (i.e. the ratio between small and large axis of the ellipsoid) of the cracks. Spherical cracks have an aspect ratio of 1 and flat cracks of less than 1. The model calculations reveal that Vp strongly decreases as a function of porosity, as observed experimentally (Weiss *et al.* 2001). This can only be caused by extremely flat cracks with an aspect ratio of about 0.005 for dry samples (Fig. 10a). At water-saturated conditions the trend given by the experimental data is slightly steeper than the modelled one for an aspect ratio of 0.005 (Fig. 10b). From the model calculations it must be expected that largely deteriorated samples (i.e. samples showing a low velocity at dry sample conditions) show a reduced Vp even at water-saturated conditions. The model-based velocity reduction for a water-saturated and a dry specimen with an average Vp of 6.49 km s^{-1} is shown in Figure 10c. It is obvious that for both, water-saturated and dry specimens, the ultrasonic wave velocities should decrease with increasing porosity when the cracks have an aspect ratio of about 0.005. This presumption is supported by the experimental data (see Fig. 10a, b) showing a similar trend of Vp_{sat} versus Vp_{dry} (Fig. 10d).

Laboratory versus field studies

On-site investigations using ultrasonic wave velocity measurements may not be easy to perform. Elastic waves propagating in rocks containing heterogeneities are affected by attenuation. The result is a loss of energy at the transducer. In the laboratory signals with a central frequency of about 1 MHz are usually used on sample with a limited size of a few centimetres. On-site inspections proved that the central frequency must be significantly lower to obtain an interpretable signal at the receiver. The difference in the central frequency has an important effect on all derived petrophysical properties. Some typical values for the central frequencies of the transducers, the wavelengths, the resolution and the maximum transmission distance in marble, both in the laboratory and in the field, are listed in Table 3.

From a theoretical point of view it is evident that the highest transmission distance is obtained at lower frequencies. However, there is a link between the transducer size and the central wavelength for a maximum efficiency in the emission and the reception of the waves. Typically the optimum value of the product of the transducer diameter (in inches) and the central frequency (in MHz) is around 0.5. For instance, a laboratory transducer of 1000 kHz has a typical diameter of 0.5 inches. As a consequence, the smaller the frequency the larger the transducer size, which is a limiting factor in practice. In fact commercial transducers used in the field have a typical central frequency of about 50 kHz and a size of about one inch, instead of the ideal value of about 10 inches. In conclusion the values for the maximum transmission distance (see Table 3) correspond to measurements under optimum conditions which are mostly not encountered on-site. Consequently the maximum transmission distance expected in the field can be significantly lower. For detailed investigations it must be considered that the spatial resolution of two individual heterogeneities also varies with the central frequency. Thus, with a frequency of about 10 kHz, a clear differentiation between two objects with a displacement of a few centimetres will not be resolved.

Conclusions

Ultrasonic wave velocity measurements are a powerful and sensitive tool for the damage assessment of marble. Thus, they may be used in a very early stage of deterioration when the rocks are apparently still intact. Water

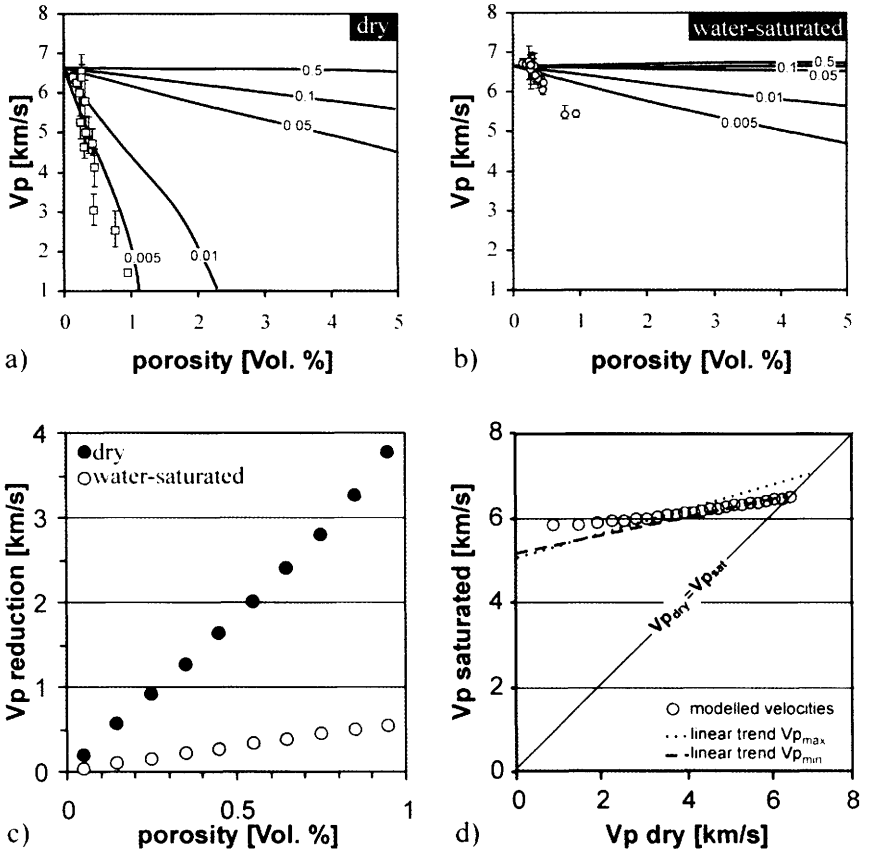

Fig. 10. Experimental versus modelled *Vp*. Velocity reduction due to microcracks with a certain aspect ratio (here 0.005, 0.01, 0.05, 0.1 and 0.5; black lines) for (**a**) dry sample conditions and (**b**) water-saturated sample conditions. Experimental data are given as average velocities (squares in (a) and circles in (b)) and their anisotropy as error bars. (**c**) Velocity reduction as a function of porosity according to the model of O'Connell & Budiansky (1974) for water-saturated and dry sample conditions and (**d**) the corresponding Vp_{sat} versus Vp_{dry} relationship. For comparison, the linear trend based on experimental data (see Fig. 9a) is given.

Table 3. *Frequency (f) dependence of some physical parameters of interest for on-site and laboratory measurements*

Physical parameter	Velocity	Field	Laboratory	
	(km s ^{1})	f = 10 kHz	f = 100 kHz	f = 1000 kHz
Wavelength	2	2 dm	2 cm	2 mm
	6	6 dm	6 cm	6 mm
Resolution	2	0.5 dm	0.5 cm	0.5 mm
	6	1.5 dm	1.5 cm	1.5 mm
Maximum transmission distance	2	20 dm	20 cm	20 mm
	6	60 dm	60 cm	60 mm

All physical parameters have been calculated for two different velocities in the material under investigation (2 and 6 km s^{-1}). The resolution parameter gives information on the maximum distance between two heterogeneities in a material which can be clearly discriminated. The maximum transmission distance is the transmission path through a sample allowing a detectable signal at the receiver position. All values are approximate.

saturation has an important influence on the magnitude and directional dependence of ultrasonic wave velocities. Hence, it is essential to gather sufficient information on the state of water saturation of an object under investigation, at least when it consists of marble.

The rock fabric determines both magnitude and directional dependence of thermal degradation. Therefore, a comprehensive knowledge of fabric properties of a marble under investigation is indispensable for a conclusive and extensive damage characterization. There exists no simple relationship between the microstructure (e.g. grain shape) and the texture (lattice preferred orientation) of marble. Thus, before using a marble on a building or as a replacement, it is essential to examine its fabric properties.

Anisotropy is the rule rather than the exception for many marbles used as natural building stones and, thus, has to be considered for conservation and reconstruction purposes as well as for on-site inspections. Anisotropy of ultrasonic wave velocities and thermal expansion are closely linked to each other. High ultrasonic wave velocities concur with small thermal expansion coefficients and small ultrasonic wave velocities with high thermal expansion coefficients. Thus, ultrasonic wave velocity measurements under water-saturated conditions give indications for intrinsic thermal expansion behaviour of a marble under investigation. This is a topic for further research for on-site application.

Enhanced understanding and quantification of the effect of thermal degradation can be achieved using theoretical models. Model calculations give important information on both the magnitude of thermal degradation and the type of thermal degradation (i.e. the possible pore geometry).

Future studies may lead to a link between short-term observations, as they are presented here, and their long-term development. The basic question to be solved is whether obvious differences in the velocity reduction due to thermally induced microcracks after only one heating cycle influence the long-term stability of marble and to what extent. When this relationship is understood, a prognosis of the lifetime of marbles may be established in advance, i.e. before utilization of a specific marble, by a simple ultrasonic screening test.

We gratefully acknowledge the constructive reviews of J. Schön and M. Prasad. This work was supported by the German Science Foundation (Grants Si 438/10-2 and Si 438/13-1). We appreciate the help with ultrasonic wave velocity measurements of M. Masson and helpful discussions with B. Zinszner and help with sampling from G. Molli.

References

ARTS, R. J., RASOLOFOSAON, P. N. J. & ZINSZNER, B. 1996. Experimental and theoretical tools for characterizing anisotropy due to mechanical defects in rocks under varying pore and confining pressures. *In*: FJAER, E., HOLT, R. M., RATHORE, J. S. (eds) *Seismic Anisotropy* (Proceedings of the 6th International Workshop on Seismic Anisotropy). Society of Exploration Geophysicists, Tulsa, 384–432.

BARSOTTELLI, M., FRATINI, F., GIORGETTI, G., MANGANELLI DEL FA, C. & MOLLI, G. 1998. Microfabric and alteration in Carrara marble: a preliminary study. *Science and Technology for Cultural Heritage*, **7**(2), 115–126.

BIRCH, F. 1960. The velocity of compressional waves in rocks up to 10 kilobars, Part I. *Journal of Geophysical Research*, **65**, 1083–1102.

BOURBIÉ, T., COUSSY, O. & ZINSZNER, B. 1987. *Acoustics of Porous Media*. Gulf, Houston.

CHRISTENSEN, N. I. 1965. Compressional wave velocities in metmorphic rocks at pressures up to 10 kilobars. *Journal of Geophysical Research*, **70**, 6147–6164.

DANDEKAR, D. P. 1968. Variation in the elastic constants of calcite with pressure. *AGU Transactions*, **49**, 323 S.

DUERRAST, H., SIEGESMUND, S. & PRASAD, M. 1999. Schadensanalyse von Naturwerksteinen mittels Ultraschalldiagnostik: Möglichkeiten und Grenzen. *Zeitschrift der deutschen geologischen Gesellschaft*, **150**(2), 359–374.

FREDRICH, J. T. & WONG, T. F. 1986. Micromechanics of thermally induced cracking in three crustal rocks. *Journal of Geophysical Research*, **91**(B12), 12743–12746.

HASHIN, Z. 1981. Analysis of Composite Materials – A Survey. *Journal of Applied Mechanics*, **50**, 481–505.

KLEBER, W. 1959. *Einführung in die Kristallographie*. VEB Verlag Technik, Berlin.

KÖHLER, W. 1991. Untersuchungen zu Verwitterungsvorgängen an Carrara-Marmor in Potsdam-Sanssouci. *In*: MÖLLER, H.-H. (ed.) *Steinschäden – Steinkonservierung*. Kolloq. im Rahmen des Kulturabkommens zw. der BRD und der DDR, Dresden, 2–6 Okt. 1989. Berichte zu Forschung und Praxis in der Denkmalpflege in Deutschland, 2, Hannover, 50–54.

LEISS, B. & WEISS, T. 2000. Fabric anisotropy and its influence on physical weathering of different types of Carrara marbles. *Journal of Structural Geology*, **22**, 1737–1745.

O'CONNELL, R. J. & BUDIANSKY, B. 1974. Seismic velocities in dry and saturated cracked solids. *Journal of Geophysical Research*, **79**(35), 5412–5426.

RASOLOFOSAON, P. N. J., RABBEL, W., SIEGESMUND, S. & VOLLBRECHT, A. 2000. Characterization of

crack distribution: fabric analysis versus ultrasonic inversion. *Geophysical Journal International*, **141**, 413–424.

REUSS, A. 1929. Berechnung der Fliessgrenze von Mischkristallen auf Grund der Plastizitatsbedingung für Einkristalle. *Zeitschrift für Angewandte Mathematik und Mechanik*, **9**, 49–58.

RUEDRICH, J., WEISS, T. & SIEGESMUND, S. 2001. Deterioration characteristics of marbles from the Marmorpalais Potsdam (Germany): a compilation. *Zeitschrift der deutschen geologischen Gesellschaft*, **152**(2–4), 637–663.

SIEGESMUND, S. 1996. The significance of rock fabrics for the geological interpretation of geophysical anisotropies. *Geotektonische Forschungen*, **85**, 1–123.

SIEGESMUND, S., ULLEMEYER, K., WEISS, T. &. TSCHEGG, E. K. 2000. Physical weathering of marbles caused by anisotropic thermal expansion. *International Journal of Earth Sciences*, **89**, 170–182.

SNETHLAGE, R., ETTL., H. & SATTLER, L. 1999. Ultraschallmessungen an PMMA-getränkten Marmorskulpturen. *Zeitschrift der deutschen geologischen Gesellschaft*, **150**(2), 387–396.

TSCHEGG, E. K., WIDHALM, C. & EPPENSTEINER, W. 1999. Ursachen mangelnder Formbeständigkeit von Marmorplatten. *Zeitschrift der deutschen geologischen Gesellschaft*, **150**(2), 283–297.

VOIGT, W. 1928. *Lehrbuch der Krystallphysik*. B. G. Teubner, Leipzig.

WEISS, T., LEISS, B., OPPERMANN, H. & SIEGESMUND, S. 1999. Microfabric of fresh and weathered marbles: Implications and consequences for the reconstruction of the Marmorpalais Potsdam. *Zeitschrift der deutschen geologischen Gesellschaft*, **150**(2), 313–332.

WEISS, T., RASOLOFOSAON, P. N. J. & SIEGESMUND, S. 2001. Thermal microcracking in Carrara Marble. *Zeitschrift der deutschen geologischen Gesellschaft*, **152**(2–4), 621–636.

WEISS, T., SIEGESMUND, S. & FULLER, E. 2002. Thermal stresses and microcracking in calcite and dolomite marbles quantified by finite element modelling. *In*: SIEGESMUND, S., WEISS, T. & VOLLBRECHT, A. (eds) *Natural Stone, Weathering Phenomena, Conservation Strategies and Case Studies*. Geological Society, London, Special Publications.

WIDHALM, C., TSCHEGG, E., EPPENSTEINER, W. 1996. Anisotropic thermal expansion causes deformation of marble cladding. *Journal of Performance of Constructed Facilities, ASCE*, **10**, 5–10.

WYLLIE, M. R. J., GREGORY, A. R. & GARDNER, L. W. 1956. Elastic wave velocities in heterogeneous and porous media. *Geophysics*, **21**, 41–70.

WYLLIE, M. R. J., GREGORY, A. R. & GARDNER, G. H. F. 1958. An experimental investigation of factors affecting elastic wave velocities in porous media. *Geophysics*, **23**, 459–493.

ZEISIG, A., SIEGESMUND, S. & WEISS, T. 2002. Thermal expansion and its control on the durability of marbles. *In*: SIEGESMUND, S., WEISS, T. & VOLLBRECHT, A. (eds) *Natural Stone, Weathering Phenomena, Conservation Strategies and Case Studies*. Geological Society, London, Special Publications, **205**, 65–80.